Catalysis Letters Vol. 102, Nos. 1–2, July 2005 (© 2005)
DOI: 10.1007/s10562-005-5201-y

On the active site in $H_3PW_{12}O_{40}/SiO_2$ catalysts for fine chemical synthesis

A.D. Newman[a], A.F. Lee[a,*], K. Wilson[a,*], and N.A. Young[b]

[a]*Department of Chemistry, University of York, York YO10 5DD, UK*
[b]*Department of Chemistry, University of Hull, Hull HU6 7RX, UK*

Received 11 January 2005; accepted 15 February 2005

The surface environment and structural evolution of silica supported phosphotungstic acid ($H_3PW_{12}O_{40}$) catalysts have been investigated as a function of acid loading. $H_3PW_{12}O_{40}$ clusters are deposited intact upon the silica surface, adopting a Stranksi-Krastanov growth mode forming a two-dimensional adlayer which saturates at 45wt% acid. Intimate contact with the silica support perturbs the local chemical environment of three tungstate centres, which become inequivalent with those in the remaining cluster, suggesting an adsorption mode involving three terminal W=O groups. Above the monolayer, $H_3PW_{12}O_{40}$ clusters form three-dimensional crystallites with physico-chemical properties indistinguishable from those in the bulk heteropoly acid. These $H_3PW_{12}O_{40}/SiO_2$ materials are efficient for the solventless isomerisation of α-pinene under mild reaction conditions. Activity scales directly with the number of accessible perturbed tungstate sites at the silica interface; these are the active species.

KEY WORDS: phosphotungstic acid; silica; α-pinene; XPS; green chemistry.

1. Introduction

Many chemical syntheses proceed through the stoichiometric application of homogeneous acids, bases or salts. This inevitably leads to the generation of large volumes of contaminated, often hazardous, waste with accompanying treatment and disposal costs. Coupled with tightening legislation on the industrial management of such toxic waste, there is a strong drive towards alternative cleaner technologies for many liquid phase fine and speciality chemical processes. One particular area offering solutions to these problems is that of heterogeneous catalysis. A number of solid or supported materials are known with high acid/base strength comparable to their currently employed homogeneous counterparts, and applicable as green replacements for undesirable homogeneous acids (e.g. H_2SO_4, $AlCl_3$, $ZnCl_2$ and BF_3).

Among the heterogeneous acid catalysts under investigation, the group of materials known as heteropoly acids (HPA) are particularly promising since they possess high Brönsted acid strengths (approaching the superacidic region) as well as tuneable redox activity depending on the particular constituent elements. Heteropoly acids are polyoxometalate inorganic cage structures, which may adopt the Keggin form with the general formula $H_3MX_{12}O_{40}$, where M is the central atom and X the heteroatom. Typically M can be either P or Si, and X = W or Mo. The highest stability and strongest acidity is observed for phosphotungstic acid ($H_3PW_{12}O_{40}$). Several review articles on the general properties and chemistry of these materials are available [1–3].

While the acid properties of heteropoly acids have excited much interest, their inherent low surface area (1–5 $m^2\ g^{-1}$) [1] often necessitates support on a porous carrier material. Neutral or acidic supports are desirable since basic materials such as alumina can decompose the HPA structure and lower the acidity of the catalysts [1,4]. Various support materials have been studied, including molecular sieves [3,5], zeolites [6,7] and activated carbon [3,4], however silica is most often used since it is widely available, is neutral or mildly acidic and possesses specific (tuneable) surface areas and porosity.

Despite the importance of developing high area, dispersed HPA catalysts, almost nothing is know about the growth mode or physico-chemical properties of polyoxometalates over silica support surfaces. It has been hypothesised that in the initial stages of impregnation, the HPA material reacts with a hydroxylated silica surface to form an ion pair with one or more silanol via simple proton transfer, possibly involving dehydration: $(\equiv SiOH_2)^+(H_2PW_{12}O_{40})^-$ [8–10] or $(\equiv Si)_m^+(H_{3-m}PW_{12}O_{40})^{m-} + mH_2O$ [8,11] However attempts to discern these surface HPA species using ^{31}P-MAS NMR (a non-surface sensitive technique) have proven inconclusive [1,3,9,11].

This work reports on the evolution of $H_3PW_{12}O_{40}$ (HPW) adlayers over a porous, hydroxylated silica using surface sensitive XPS coupled with Raman, IR and XRD. We identify a unique interfacial tungstate environment within the HPW cage which is responsible for

* To whom correspondence should be addressed.
E-mails: afl2@york.ac.uk, kw13@york.ac.uk

catalytic activity in the environmentally benign, liquid phase rearrangement of α-pinene; an important process in the fragrance and flavourings sectors.

2. Experimental

2.1. Catalyst preparation

A series of phosphotungstic acid catalysts were prepared with loading over the range 0.3–63wt% HPW/SiO_2. Simple wet impregnation was employed, involving dissolution of the required amount (0.05–9 g) of $H_3PW_{12}O_{40}$ (Aldrich, 70.1wt% W) in 50 ml methanol in a round-bottomed flask, followed by addition of between 2.5 and 10 g of silica powder support material (Fisher 100 Å). The resulting mixture was left overnight followed by evaporation to a dry, free flowing powder at ~60 °C under vacuum. No further pre-treatments were applied to any catalysts, which were stored in air prior to analysis and reaction testing.

2.2. Bulk characterisation

Elemental analysis was undertaken on a Fisons ICP-OES instrument, with water content (both physisorbed and crystalline) calculated by thermal gravimetric analysis (TGA) using a Stanton Redcroft STA-780 between 20 and 700 °C. Nitrogen porosimetry measurements were performed on Micromeritics ASAP2010 instrument. Surface areas were calculated using the BET equation over the range $P/P_0 = 0.02–0.2$, where a linear relationship was maintained, while pore size distributions were calculated using the BJH model up to $P/P_0 = 0.6$. Approximate calculation of the monolayer coverage is based on the average area per anion for the (100) planes of 2D arrays on HOPG and of that for the bulk $H_3PW_{12}O_{40}$ structure of 144 $Å^2$ [12]. DRIFT spectra were obtained using a Bruker Equinox FTIR spectrometer. Samples were diluted with KBr powder (2wt% in KBr), then loaded into an environmental cell and subjected to a vacuum at 70 °C prior to measurement. FT-Raman spectra were collected in 180 ° scattering geometry from neat samples using a Bruker FRA 106/S Raman module mounted on a Bruker Equinox 55 FTIR bench with a cw Nd-YAG 1064 nm laser operating at 100–400 mW, a CaF2 beamsplitter and liquid nitrogen cooled Ge detector.

2.3. X-ray photoelectron spectroscopy

XPS measurements were performed using a Kratos AXIS HSi instrument equipped with a charge neutraliser and MgK_α X-ray source. Spectra were recorded at normal emission using an analyser pass energy of 20 eV, and X-ray power of 225 W. Energy referencing was employed using the valence band. Spectra were Shirley background-subtracted across the energy region and fitted using CasaXPS Version 2.1.9. A common line shape was adopted for each element, based on a Doniach-Sunjic mix, with FWHM = 1.7 (W 4*f*), 2.1 (Si 2*p*), 2.1 (O 1*s*), and asymmetry factors = 0.0007 (W), 0.063 (Si), 0.04 (O), respectively.

2.4. Reactivity

α-Pinene isomerisation was performed using a Radley's carousel reaction station under air at 30 °C. Hundred milligram of air-exposed catalyst were added to 63 mmol of α-pinene (98%, Aldrich), with 0.1 cm^3 of tetradecane (99%, Lancaster) added as internal standard. Stirred reactions were run for 24 h. Samples were analysed by a Varian CP-3800 gas chromatograph with CP-8400 autosampler using a Carboxen 1006 Plot column (30 m × 0.53 film). The principal major products were camphene and limonene, along with traces of terpinene, para-cymene and terpinolene in accordance with literature [13,14]. Catalyst selectivity and overall mass balances (closure was >98%) were determined using appropriate reactant and product response factors derived from multi-point calibration curves. The systematic errors in conversions and selectivities are ±2% and ±3%.

3. Results and discussion

3.1. HPW growth mode

The successful impregnation of silica by the HPW precursor was first examined via elemental analysis (figure 1). Bulk analysis was consistent with the progressive incorporation of increasing HPW into the final materials with nominal HPW loading. The P : W atomic ratio remained approximately constant across the series at ~1:12 in excellent agreement with that of the parent 12-phosphotungstic acid. The surface W coverage also rose as a function of HPW loading, but reached a plateau of around 10wt% W for loadings in excess of 44wt% suggestive of monolayer saturation (as discussed later). Additional heteropoly acid incorporated onto the

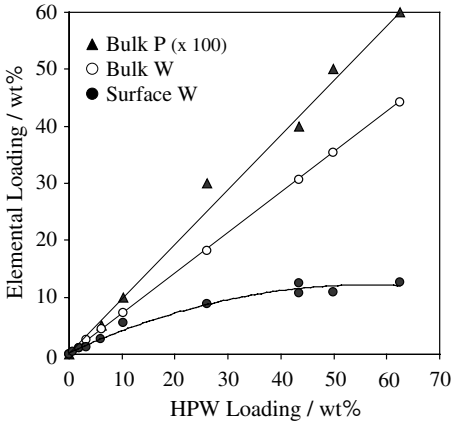

Figure 1. Bulk and surface elemental analysis of HPW/SiO_2 series.

silica support at higher loadings, evidenced from the rising bulk W content, must therefore serve to encapsulate and screen the XP contribution from the initially deposited phase – indicative of multilayer or three-dimensional crystallite growth.

Porosimetry measurements revealed a gradual reduction in both surface areas and pore volume with increasing HPW loadings (table 1). However the average pore diameter remained constant between 130 and 140 Å, suggesting the heteropoly acid phase remains well dispersed even for loadings upto 45wt% which still retain surface areas of 130 $m^2\ g^{-1}$. STM and XRD measurements on bulk and graphite supported $H_3PW_{12}O_{40}$ heteropoly acids reveal the average surface area occupied per Keggin anion is 144 Å [12] . The theoretical surface area of a 2D HPW adlayer can be calculated using this value and is also shown in table 1 as a function of the HPW loading. It is immediately apparent that a fully dispersed $H_3PW_{12}O_{40}$ film would completely cover the silica support for loadings >44%, in good accordance with the XPS results. In other words, the heteropoly acid spreads continuously across the silica surface upto a loading of ~44wt% HPW, which saturates the monolayer. Higher $H_3PW_{12}O_{40}$ loadings resulted in a dramatic loss of surface area and associated pore blockage, indicating a change in growth mode and bulk HPW agglomeration (see later).

3.2. Evolution of surface species

The nature of the surface species present in the low (monolayer) and high (multilayer) loading regimes was explored by surface spectroscopies and powder XRD.

Evolution of the surface tungstate environment as a function of HPW loading was first followed via XPS. The resulting W 4*f* XP spectra are shown in figure 2 and are characteristic of high oxidation state tungstate environments which span ~33–36 eV. These spectra reveal a broad, poorly resolved doublet centred around 35.3 eV ($4f_{7/2}$ component), consistent with that in the pure parent $H_3PW_{12}O_{40}$ heteropoly acid, together with a low binding energy (BE) shoulder at 33.8 eV. A deconvoluted spectrum for the 44wt% HPW sample is shown inset. The high BE state evolves linearly with HPW coverage upto 44wt%, beyond which its intensity and resolution increase dramatically, resulting in a spin-orbit splitting of ~2.2 eV (identical to that of bulk $H_3PW_{12}O_{40}$). The low BE state likewise increases almost linearly with HPW coverage, but reaches a maximum at the nominal monolayer point being rapidly attenuated at higher HPW loadings. The loading dependencies of both tungstate surface species are shown in figure 3, and clearly mirror each other during the monolayer regime. The bulk-like HPW moiety dominates the perturbed tungstate chemical environment by a constant factor of ~3:1 during evolution of the monolayer. The relative contributions from these states only deviate once multilayer/crystallite growth commences; rapid attenuation of the low BE tungstate reveals this species is associated with the silica interface.

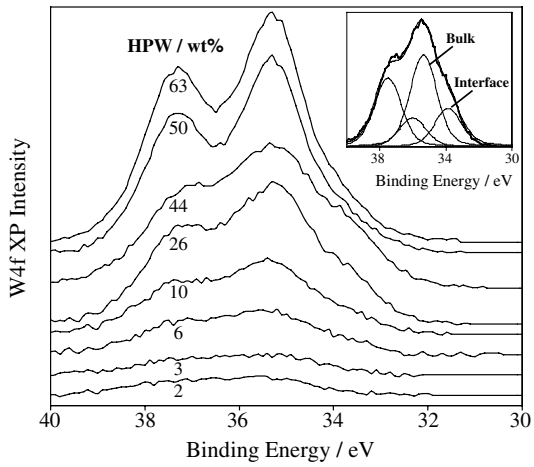

Figure 2. W 4*f* XP spectra of HPW/SiO_2 series as a function of HPW loading. Inset shows deconvoluted components for the 44wt% sample using a common lineshape.

There are two clear possibilities for the origin of these distinct W environments: either some of the HPW decomposes over the silica support yielding a mixed adlayer of intact Keggin units and a discrete WO_X phase; or the monolayer consists solely of intact Keggin units which contain inequivalent W atoms. Measure-

Table 1
Porosimetry results for HPW/SiO_2 series

Wt% HPW	BET surface area ($m^2\ g^{-1}$)	BJH pore volume ($cm^3\ g^{-1}$)	Average pore diameter (Å)	Theoretical surface coverage ($m^2\ g^{-1}$)	Monolayer fraction (%)
0 (silica)	387.6	1.42	142.9	0	0
1.9	318.5	1.16	142.3	5.7	2
3.6	302.1	1.1	137.6	9.6	3
5.9	297	1.13	149.4	17.8	5
10.3	234.8	0.88	139.6	31	13
26	186.2	0.70	151.1	78	42
43.5	132.8	0.58	151.9	135	102
49.9	95.7	0.35	145.2	150	157
62.5	57.2	0.20	132.3	189	330

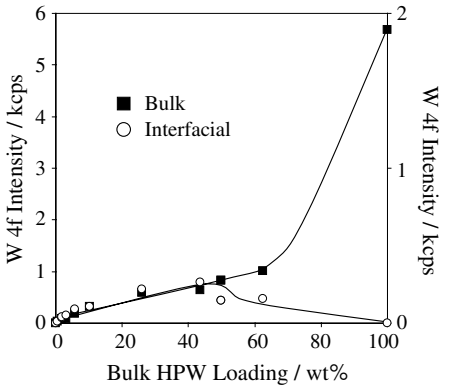

Figure 3. Fitted intensities of deconvoluted W 4*f* XP components as a function of HPW loading.

ments on a WO_3 standard revealed a well-resolved doublet with $4f_{7/2}$ BE of 34.4 eV, distinct from either species observed upon HPW impregnation. Although this observation favours the latter interpretation, the nature of the surface tungstate species was further investigated by the powerful combination of DRIFTS and Raman vibrational spectroscopies.

DRIFTS measurements on the submonolayer HPW loaded samples gave rise to the expected peaks for phosphate, tungstate and silicate groups [6,9,15] (figure 4a). For the lowest loadings the asymmetric W–O–W stretch at 800 cm^{-1} is masked by a strong Si–O–Si band from the underlying substrate, however the corresponding internal W–O–W stretching mode ~895 cm^{-1} clearly grows in with HPW coverage and saturates at ~44wt% (the monolayer point). These changes are accompanied by progressive attentuation of both siloxane and silanol features at 800/1100 and 970 and 3700 cm^{-1}, respectively, and the emergence of terminal W=O stretches ~1000 cm^{-1} and the asymmetric P–O stretch at 1080 cm^{-1}. Hence characteristic HPW vibrations are apparent throughout the evolution of both mono- and multilayer surface phases.

The analogous Raman spectra strongly support this finding (figure 4b), with bands characteristic of the external W–O–W symmetric and asymmetric stretches of HPW [15,16] at shifts of 533 and 900 cm^{-1}, and intense bands characteristic of terminal W=O stretches at 990 and 1005 cm^{-1}. Although it is difficult to distinguish the weaker features at the lowest loadings, the Raman spectra of the saturated monolayer bears a striking resemblance to that of the pure HPW. There was also no evidence for the extremely intense fingerprint WO_3 bands at 716 and 805 cm^{-1} from any of the samples. The DRIFTS and Raman therefore provide strong support for the formation of a uniform HPW monolayer across the silica support without significant degradation.

Final confirmation of the gradual evolution of a pure HPW adlayer was provided by XRD. Figure 5 shows the only crystalline phase present for all loadings corresponded to $H_3PW_{12}O_{40}$ [17,18]. There were no reflections present due to WO_3 formation.

Together these observations evidence the continuous two-dimensional growth of a homogeneous HPW monolayer across the support with increasing loading. Despite their similarity to the parent heteropoly acid, the HPW phase contains two distinct tungstate environments when supported within the monolayer, reverting back to a single, bulk-like environment within the multilayers. The only way to reconcile these findings is if some of the W atoms within the Keggin units are perturbed by proximity to the SiO_2; essentially the introduction of a surface breaks the molecular symmetry within the $H_3PW_{12}O_{40}$ cluster. Those terminal W=O groups coordinating to the surface ("facing down") will experience more efficient core-hole screening than the remainder, reducing final state contributions and thus lowering their W 4f BE relative to those W=O groups "facing away" which reside in a bulk-like environment. Indeed the ratio of bulk : perturbed W atoms of ~3:1 is consistent with an adsorption geometry in which each Keggin unit binds to the silica through 3 terminal W=O

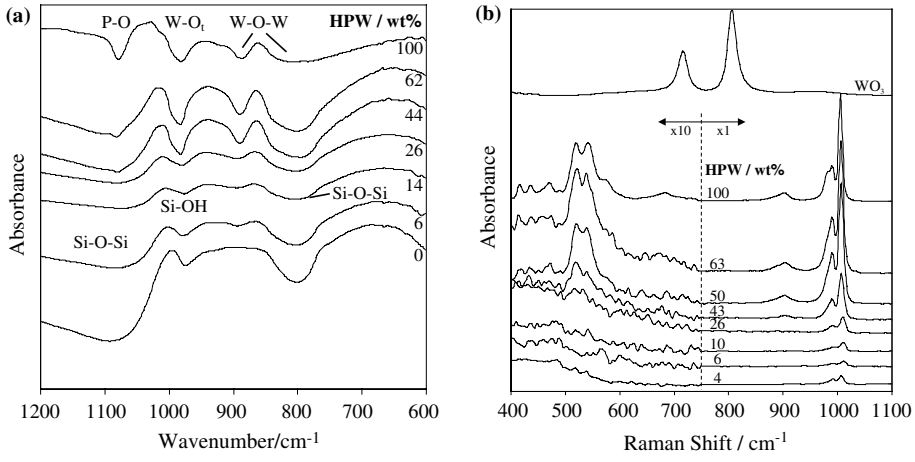

Figure 4. (a) DRIFT and (b) Raman spectra of HPW/SiO_2 series as a function of HPW loading. Comparative spectra for pure WO_3 are also shown.

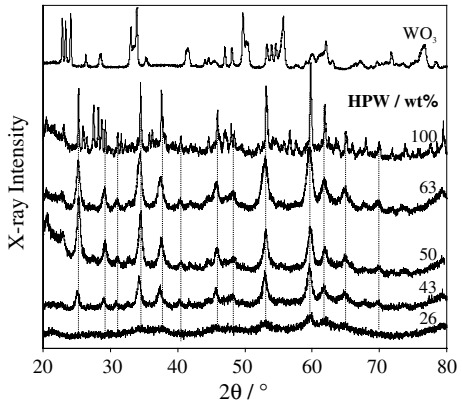

Figure 5. Powder X-ray diffractograms of HPW/SiO_2 series as a function of HPW loading. A comparative diffraction pattern for pure WO_3 is also shown.

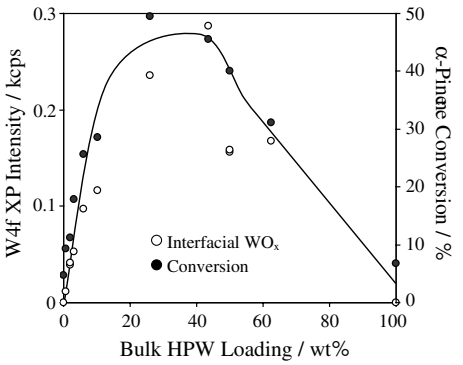

Figure 6. Correlation between α-pinene conversion and surface coverage of interfacial HPW tungstate centres for HPW/SiO_2 catalysts.

bonds. Whilst interactions of this type have been speculated [8,11] this represents the first spectroscopic evidence in support of such a bonding mode.

3.3. Active site in α-pinene isomerisation

The liquid phase isomerisation of α-pinene was subsequently explored as a function of HPW loading in order to both test the catalytic utility of these materials and to shed insight into the chemical properties of the surface HPW species. Figure 6 shows the resulting α-pinene conversion to monocyclic products (predominantly limonene with residual terpinolene) across the $H_3PW_{12}O_{40}/SiO_2$ series. Neither the bare silica support or pure, unsupported HPW showed significant reactivity above the background rate with <7% conversion after 24 h. Conversion rose sharply with increasing HPW loading within the monolayer regime, passing through a maximum at around 45% α-pinene conversion, before falling dramatically at higher (multilayer) loadings. This volcano dependence of the catalytic performance on loading shows a striking correlation with the surface coverage of exposed W=O centres coordinated to the silica support. These are the electronically perturbed sites which accumulate during growth of the HPW monolayer due to interaction with the silica surface, and which become encapsulated, and inaccessible to reactants, upon multilayer "bulk" HPW formation. In summary α-pinene isomerisation unequivocally occurs at these interfacial tungstate sites.

4. Conclusions

A series of $H_3PW_{12}O_{40}/SiO_2$ catalysts were prepared via simple wet impregnation spanning a wide loading range. The HPW phase is deposited intact and grows continuously across the silica support to form a homogeneous, two-dimensional monolayer film which saturates around 45wt% $H_3PW_{12}O_{40}$. Higher loadings results in the formation of a bulk-like, three-dimensional HPW phase. The physico-chemical properties of tungstate species within the Keggin cluster are perturbed by close proximity to the silica surface. $H_3PW_{12}O_{40}$ units appear to coordinate to silica through 3 terminal W=O linkages, which exhibit high activity towards the isomerisation of α-pinene.

Acknowledgments

Financial support by the UK Engineering and Physical Sciences Research Council under grants GR/M20877/01 and GR/R39436/01, and from BP Chemicals is gratefully acknowledged.

References

[1] I.V. Kozhevnikov, Catal. Rev. Sci. Eng. 37(2) (1995) 311.
[2] M.T. Pope, *Heteropoly and Isopoly Oxometalates* (Springer-Verlag, Berlin, 1983).
[3] I.V. Kozhevnikov, Chem. Rev 98 (1998) 171.
[4] Y. Izumi and K. Urabe, Chem. Lett. (1981) 663.
[5] K. Nowińska, R. Fórmaniak, W. Kaleta and A. Waclaw, Appl. Catal A: Gen. 256 (2003) 115.
[6] K. Pamin, A. Kubacka, Z. Olejniczak, J. Haber and B. Sulikowski, Appl. Catal. A: Gen. 137 (2000) 194.
[7] E. López-Salinas, J.G. Hernández-Cortéz, I. Schifter, E. Torres-García, J. Navarrete, A. Gutiérrez-Carrillo, T. López, P.P. Lottici and D. Bersani, Appl. Catal. A: Gen. 193 (2000) 215.
[8] I.V. Kozhevnikov, K.R. Kloetstra, A. Sinnema, H.W. Zandbergen and H. Bekkum, J. Mol. Catal. A: Chem. 114 (1996) 287.
[9] T. Blasco, A. Corma, A. Martínez and P. Martínez-Escolano, J. Catal 177(2) (1998) 306.
[10] F. Lefebvre, J. Chem. Soc. Chem. Comm. (1992) 756.
[11] V.M. Mastikhin, S.M. Kulikov, A.V. Nosov, I.V. Kozhevnikov, I.L. Mudrakovsky and M.N. Timofeeva, J. Mol. Catal. 60(1) (1990) 65.
[12] M.S. Kaba, I.K. Song, D.C. Duncan, C.L. Hill and M.A. Barteau, Inorg. Chem. 37 (1998) 398.
[13] G. Gündüz, R. Dimitrova, S. Yilmaz, L. Dimitrov and M. Spassova, J. Mol. Catal. A: Chem. 225(2) (2004) 253.
[14] M.A. Ecormier, K. Wilson and A.F. Lee, J. Catal. 215(1) (2003) 57.

[15] R. Thouvenot, M. Fournier, R. Franck and C. Rocchiccioli-Deltcheff, Inorg. Chem. 23 (1984) 598.
[16] W. Kuang, A. Rives, M. Fournier and R. Hubaut, Appl. Catal. A: Gen. 250 (2003) 221.
[17] B.B. Bardin and R.J. Davis, Appl. Catal. A: Gen. 200 (2000) 219.
[18] I.V. Kozhevnikov, S. Holmes and M.R.H. Siddiqui, Appl. Catal. A: Gen. 214 (2001) 47.